I J C T A, 9(38), 2016, pp. 307-322

Dynamic Model for Wind Farms with Fixed Speed Induction Machine: Case Study of Wind Farms of Sidi-Daoud in Tunisia

R. Karoui*, H. Khadraoui and F. Bacha*

ABSTRACT

A wind farm is generally composed of a large number of wind turbines which implies a large order system. This order weighed down strongly the calculation and simulation time. Indeed, to assess wind farm behavior, it is normal practice to use aggregate models in which the units are replaced by a single equivalent unit. This paper represents the aggregation procedures of a wind farm (already mentioned in several references). This aggregation is checked by a case of application on the Sidi-Daoud wind farm northeast of Tunisia. This wind farm is composed by fixed-speed wind turbines using squirrel cage induction generators (SCIG). Our work begins with identification of the wind farm of Sidi-Daoud then the modeling of the wind turbine system thereafter the aggregation procedures of a wind farm. Finally, we conclude by simulations before and after aggregation for a Weibull wind model under Power System Analysis Toolbox (PSAT) software.

Keywords: Wind farm, wind turbine, wind model, Weibull model, power system analysis.

1. INTRODUCTION

Wind energy has become an important factor in the energy strategy of a large number of countries. This importance comes from the fact that these energy resources are abundant and non-polluting. Also, this energy represents to long term a significant economic gain and contributes to the equilibrium of energy balance. Tunisia is among the countries that have wanted to profit of these abundant energy resources, therefore, it was created the first wind power farm in the region of Sidi-Daoud north east of the country in cooperation with the Spanish company MADE. This wind farm consists of 70 wind turbines of total power 53.6 MW installed in three steps, the first step began production in 2000 [1]. This wind farm consists of fixed speed wind turbines based on squirrel cage induction generators (SCIG).

In this paper, we focus on the aggregation of the third step (step C) of wind farm of Sidi-Daoud which consists of 26 wind turbines of same type (AE61) of total power 34.32 MW. This aggregation has the advantage of reducing the system order which is generally very high and therefore allows easy programming and minimize the simulation time. In this work we began with a presentation of the wind farm of Sidi-Daoud then a modeling of different constituents of a wind turbine system (based on a asynchronous cage machine) thereafter, we present the wind farm aggregation procedures [3, 5, 9, 11] and finally, we conclude by simulations before and after aggregation for a Weibull wind model under Power System Analysis Toolbox (PSAT) Software. Some recent control methods are discussed in [15-22].

2. PRESENTATION OF SIDI-DAOUD WIND FARM

This wind farm includes 70 wind turbines with approximately a total power 54 MVA. These wind turbines are installed in three steps (A, B and C) and completed in 2009, details of which are given by the Table 1.

* University of Tunis, ENSIT, Tunis, Tunisia.

Table 1
Wind farm of Sidi-Daoud

	Step A (Phase A)	Step B (Phase B)	Step C (Phase C)
Number of Wind Turbines	32	12	26
Installed power (MW)	10.560	8.720	34.320
Date of Service	August 2000	September 2002	June 2009
Constrictor	MADE Spain	MADE Spain	MADE Spain
Annual production (GWh)	28	20	100

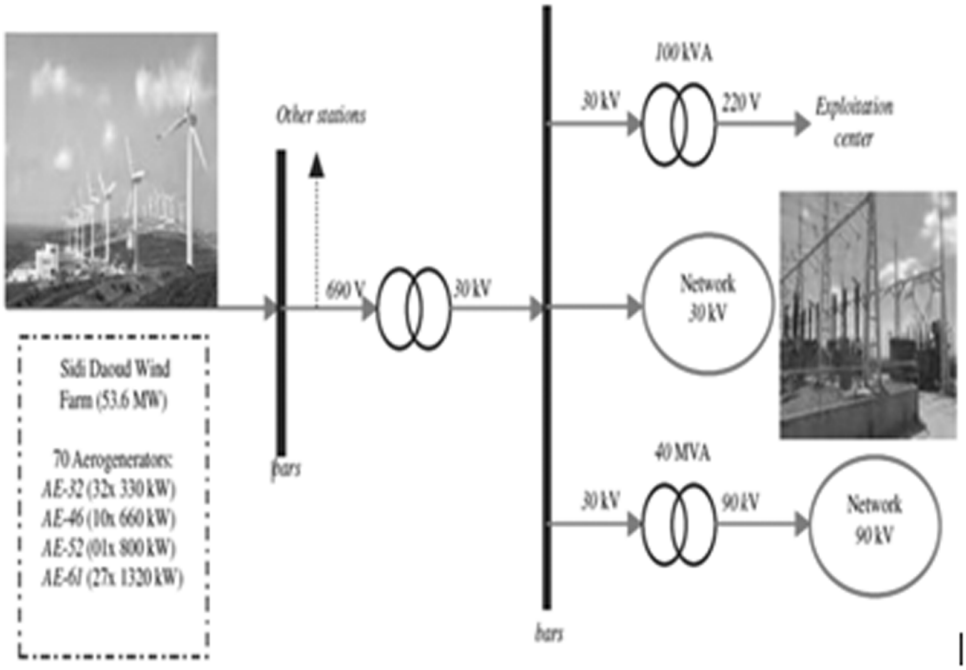

Figure 1: Connection of Sidi-Daoud wind farm to the grid

Figure 1 shows the connection of the Sidi-Daoud wind farm to the electrical distribution network.

3. CONNECTION OF THE WIND TURBINE TO THE GRID

Figure 2 shows the connection of a fixed-speed wind turbine (using SCIG) to the grid. The rotor speed of the generator is fixed independently of the wind speed and is determined by the frequency imposed by the network, gear ratio and generator design [8]. The machine magnetization is ensured by a capacitors battery. The generator is directly connected to the network via a soft starter (the exchanged powers are not controlled).

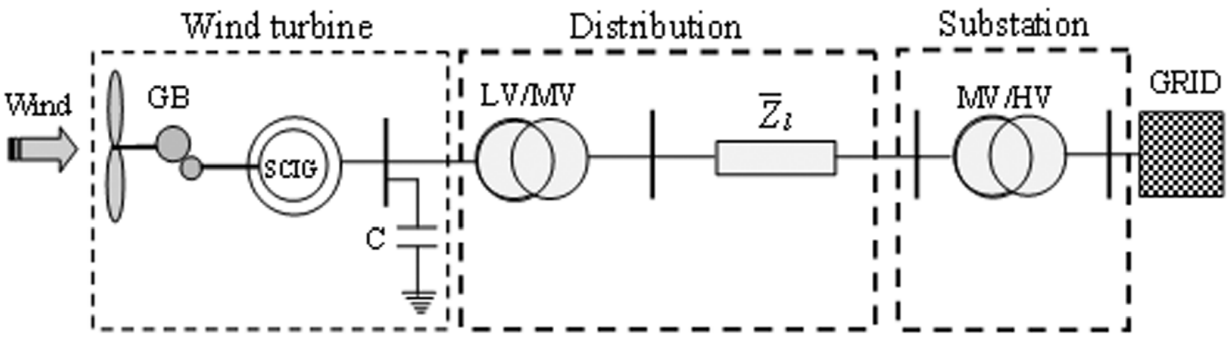

Figure 2: Fixed speed wind turbine connected to grid

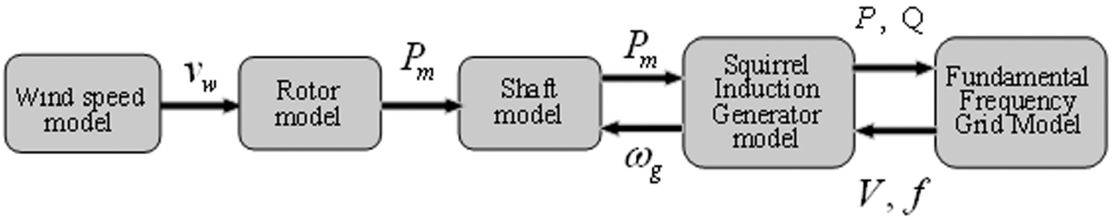

Figure 3: Model of constant speed wind turbine

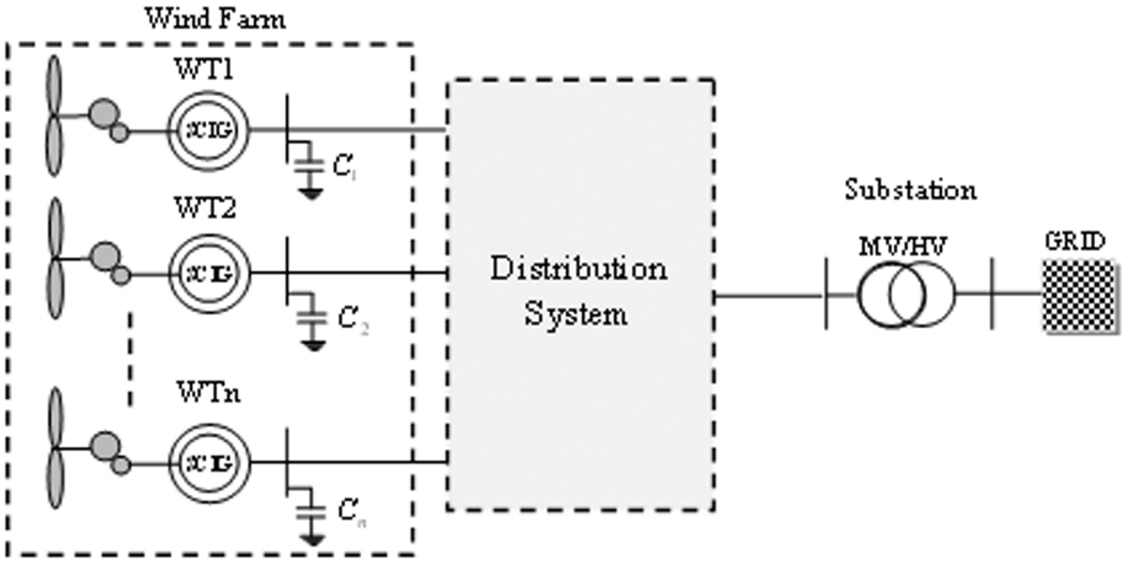

Figure 4: Connection of a wind farm to the grid

Figure 4 shows a wind farm connected to the grid via a distribution system. This system consists of the transformers LV / MV and the connection lines to the substation MV / HV.

4. AERODYNAMIC MODEL

For a fixed speed wind turbine, the mechanical power available on the shaft of a wind turbine is determined analytically by the following equation:

$$P_W = \frac{1}{2}\rho . C_p(\lambda).\pi . R^2 . v_w^3 \tag{1}$$

where R is the radius of the turbine (blade) and ρ is the air density ($kg.m^{-3}$), the power coefficient $C_p(\lambda)$ which depends on the speed ratio λ (speed ratio) is defined as follows:

$$C_p = 0.44\left(\frac{100}{\Lambda} - 5.4\right)e^{-\frac{13.5}{\Lambda}} \tag{2}$$

with:

$$\Lambda = \frac{1}{\frac{1}{\lambda} + 0.002}$$

and:

$$\lambda = \frac{v_t}{v_W} = \frac{\omega_t . R}{v_W} \tag{3}$$

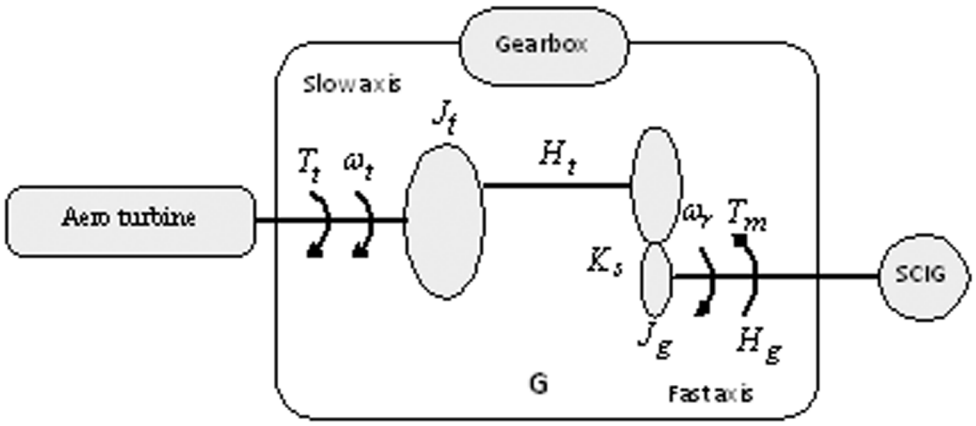

Figure 5: Two-mass model of the gear box

5. TRANSMISSION SYSTEM MODEL

In transient stability studies, the most widely used drive train model is the two-mass model. The first mass is composed by the turbine and slow shaft and the second mass is composed of the fast shaft and a generator.

The dynamics of the two-mass model takes into account the rotor inertia H_i and the machine rotor inertia H_g and the torsion coefficient of low speed shaft K_s. The dynamic model is given by the following dynamic equations:

$$\begin{cases} \dfrac{d\omega_t}{dt} = \dfrac{T_t - K_S.\theta_{ta}}{2H_t} \\ \dfrac{d\omega_r}{dt} = \dfrac{K_S.\theta_{ta} - T_m}{2H_g} \\ \dfrac{d\theta_{ta}}{dt} = \omega_b(\omega_t - \omega_r) \end{cases} \tag{4}$$

Here:

$$\theta_{ta} = \theta_t - \theta_r$$

where T_m and T_t and e T are the mechanical and turbine torque, respectively; ω_t and ω_r are the turbine and generator speed; θ_{ta} is the twist angle.

6. GENERATOR MODEL

In our study of aggregation, we use the two models of the asynchronous machine namely the steady state model used of parameters of the induction machine estimation and the equivalent dynamic model for transient response.

6.1. Steady state model

The generator model is similar to a squirrel cage induction motor. The only difference with respect to the induction motor is that the currents are positive if they are injected into the network. With the notations adopted for the parameters asynchronous machine and which are given as follows:

$$X_S = L_S.\omega_S; \quad X_r = L_r.\omega_S; \quad X_m = M.\omega_S; \quad x_S = X_S - X_m; \quad x_r = X_r - X_m.$$

The steady state model of the induction machine is represented by Figure 8.

This representation is very useful for identification of parameters of equivalent generator of aggregated model of wind farm.

6.2. Dynamic model

In dynamic model given by Figure 6, the equivalent circuit of the SCIG is characterized by a transient e.m.f. in series with transient impedance. This model is called synchronous model of the asynchronous machine. This model is a standardized representation for power system stability studies.

The differential equation of model frequently used is third order model represented in the synchronous reference frame which takes into consideration the transient e.m.f. and the slip [6, 13].

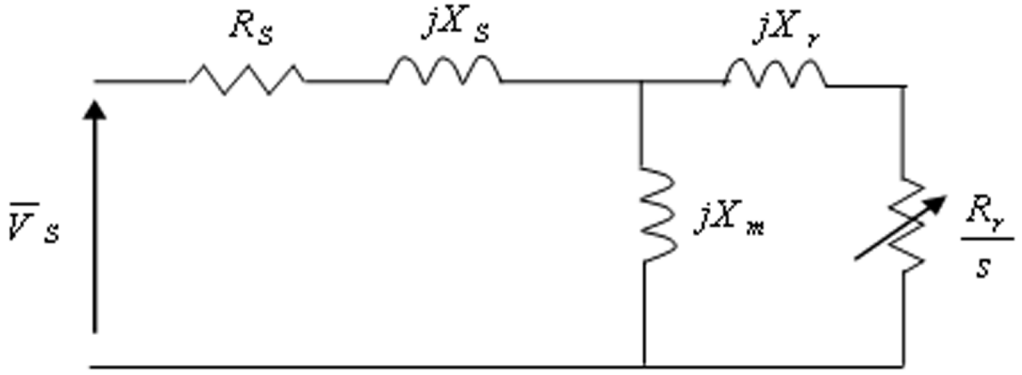

Figure 6: Equivalent circuit of the Steady state Model of SCIG

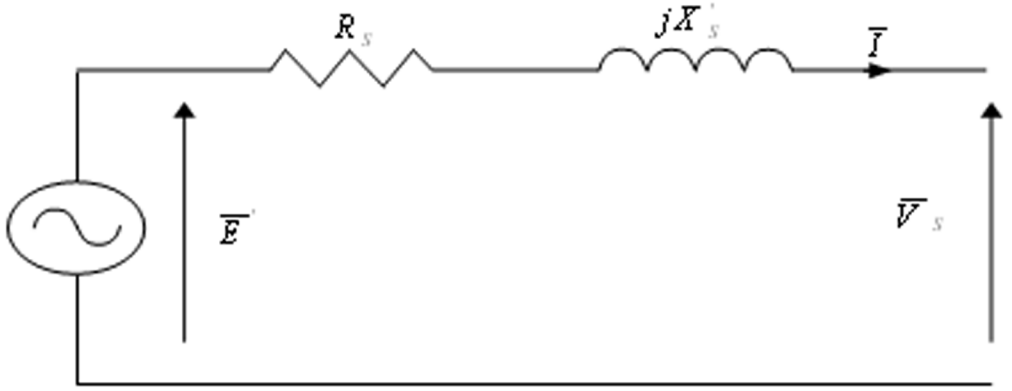

Figure 7: Transient model of induction generator

$$\begin{cases} \dfrac{dE'_d}{dt} = -\dfrac{1}{T'_0}.[E'_d - (X_S - X'_S).I_{qs}] + s.\omega_S.E'_q \\ \dfrac{dE'_q}{dt} = -\dfrac{1}{T'_0}.[E'_q - (X_S - X'_S).I_{ds}] + s.\omega_S.E'_d \\ \dfrac{ds}{dt} = \dfrac{T_e - T_m}{2\left(H_t + H_g\right)} \end{cases} \quad (5)$$

where:

$$X_s^{'} = X_s - \frac{X_m^2}{X_r} \tag{6}$$

S is the slip defined as follows:

$$s = \frac{\omega_S - \omega_r}{\omega_S} \tag{7}$$

$T_0^{'}$ The transient time constant,

$$T_0^{'} = \frac{X_r}{\omega_S R_r} \tag{8}$$

The electrical torque is:

$$T_e = E_d^{'}.I_{ds} + E_q^{'}.I_{qs} \tag{9}$$

7. WIND FARM AGGREGATION

For the steady-state and transient studies, a wind farm is similar to a conventional thermal power plant composed of several identical generating units. To assess its behavior it is practice to use aggregate models in which the units are replaced by a single equivalent unit. Generally a large wind farm is divided into several groups of wind turbines depending on their types and the wind profile. Each group is connected to a common bus and the set is connected to the network bus.

The aggregation must be carried out in several steps as shown by the Figure 8.

There are several hypotheses in the literature that facilitate the aggregation of a wind farm and that we have summarized in essential six hypotheses to know [3, 7, 8].

- For each wind turbines group, the wind speed is considered to be uniform and of same turbulence level;
- The wind turbines of the same group have to be connected in parallel to the same bus;

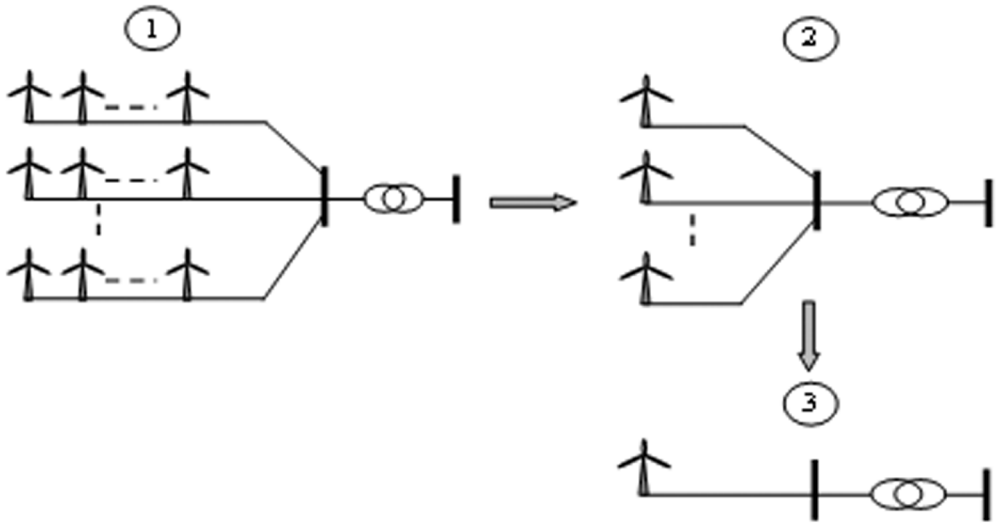

Figure 8: The steps of aggregation

- The wind turbines to aggregate have to be of same type;
- The equivalent machine parameters correspond to the parallel combination of WGs;
- Wind turbines must possess the same distribution system (cable and transformer) connected to the common bus;
- The lines and transformers of distribution system in the wind farm should be grouped in parallel.

The fundamentals of the aggregate model can be symbolically expressed by the following set of equations:

$$S_{eq} = \sum_{i=1}^{n} S_i;\ C_{eq} = \sum_{i=1}^{n} C_i;\ V_{eq} = \frac{1}{n}\sum_{i=1}^{n} v_i(t);\ H_{eq} = \sum_{i=1}^{n} H_i$$

where n is the total number of wind turbines to aggregate.

S : Nominal power;

C : Capacitance of the reactive power compensation system;

V_{eq} : Mean wind speed;

H : Inertia constant of turbine and generator.

8. GENERATORS AGGREGATION

The generators are assumed connected in parallel. We may define the equivalent impedances, stator, rotor and mutual [5].

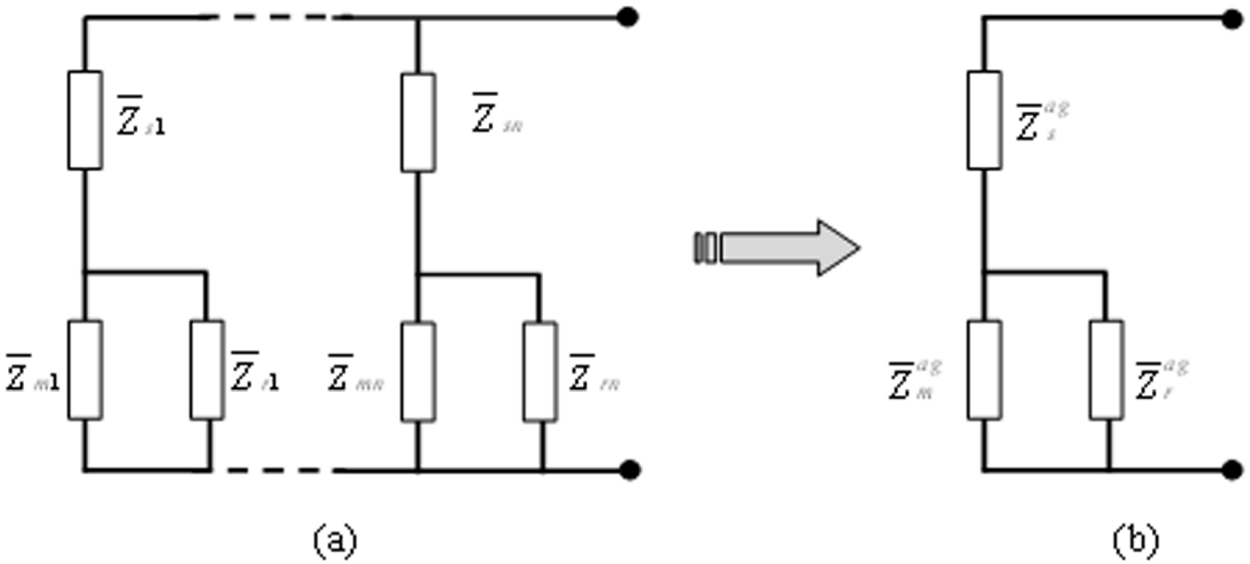

Figure 9: Generators aggregation

Figure 9 (a) shows the parallel connection of equivalent diagram of generator of wind turbines connected to a common bus before aggregation; the Figure 9 (b) shows the equivalent diagram after aggregation.

$$\overline{Z}Si = R_{Si} + jX_{Si};\ \overline{Z}ri = \frac{R_{ri}}{s} + jX_{ri};\ \overline{Z}mi = jX_{mi} \tag{10}$$

$$\overline{Z}eqi = \overline{Z}Si + \frac{\overline{Z}mi.\overline{Z}ri}{\overline{Z}mi + \overline{Z}ri} \tag{11}$$

All wind turbines are of the same type, so we can write:

$$\overline{Z}eq1 = \overline{Z}eq2 = ... = \overline{Z}eqi = ... = \overline{Z}eqn = \overline{Z}eq$$

The aggregate impedance is given as follows:

$$\overline{Z}_{eq}^{agg} = \frac{\overline{Z}eq}{n} = \frac{\overline{Z}S}{n} + \frac{\overline{Z}m.\overline{Z}r}{n.(\overline{Z}m + \overline{Z}r)} \tag{12}$$

8.1. Distribution network aggregation

The total impedance of equivalent line is given by the following expression:

$$\overline{Z}eq = \frac{(\sum_{i=1}^{n} \overline{Z}i.m_i^2)}{(\sum_{i=1}^{n} m_i)^2} \tag{13}$$

where $\overline{Z}i$ is the line impedance of the branch i and m_i is the wind turbine number in the branch i.

For the shunt capacitance of line, the equivalent susceptance is expressed as follows:

$$B_{eq} = \sum_{i=1}^{n} B_i \tag{14}$$

The LV/MV transformers are also considered connected in parallel; their equivalent impedance is given as follows.

$$\overline{Z}tr_{eq} = \frac{\overline{Z}tr}{n}$$

8.2. Equivalent dynamic model

The equivalent dynamic model is illustrated in the following figure:

According to this representation (Figure10 (a)), we can calculate the equivalent Thevenin model of aero-generators saw of connection bus (Figure10 (b)). The total current injected to the connection bus of all aero-generators is given by:

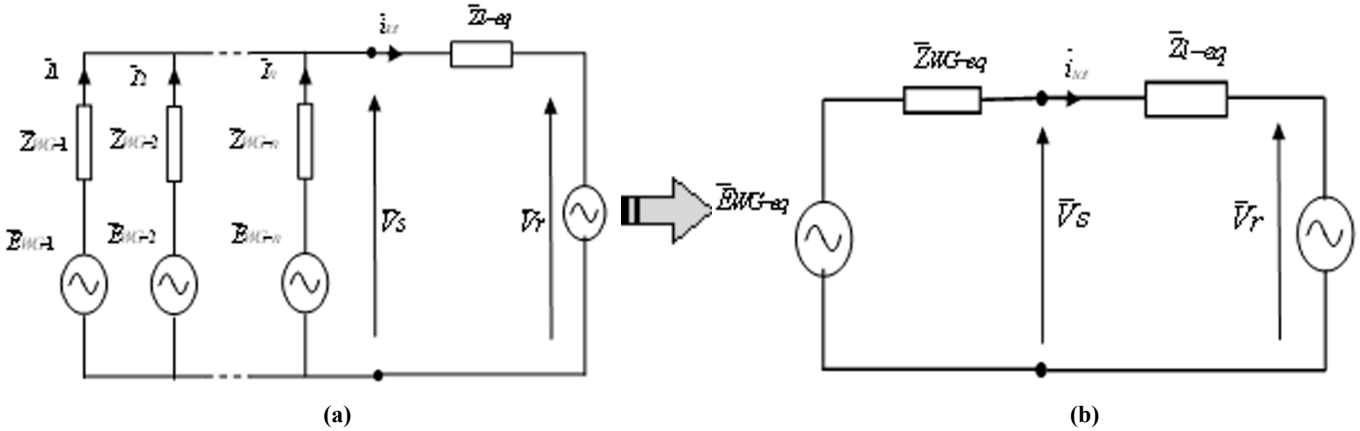

(a) (b)

Figure 10: Thevenin equivalent of the aero-generators

$$i_{bus} = \sum_{i=1}^{n} i_{WG_i} = \sum_{i=1}^{n} \frac{(\overline{E}WG_i - \overline{V}r)}{\overline{Z}i_{tot}} \tag{15}$$

In terms of admittance, we can write:

$$i_{bus} = \sum_{i=1}^{n} \overline{Y}i_{tot} .(\overline{E}WG_i - \overline{V}r) \tag{16}$$

$$\overline{K}WG_i = \frac{\overline{Y}i_{tot}}{\sum_{i=1}^{n} \overline{Y}i_{tot}} = \frac{\overline{Y}i_{tot}}{\overline{Y}Th} \tag{17}$$

Developing the equation (*p*), we obtain:

$$\bar{i}bus = \overline{Y}Th . \sum_{i=1}^{n} \overline{K}WG_i . \overline{E}WG_i - \overline{V}r \sum_{i=1}^{n} \overline{Y}i_{tot} \tag{18}$$

which gives:

$$\bar{i}bus = \overline{Y}Th .(\sum_{i=1}^{n} \overline{K}WG_i . \overline{E}WG_i - \overline{V}r) \tag{19}$$

Ultimately the Thevenin equivalent model of the wind farm and given by the following equations:

$$\begin{cases} \overline{E}Th = \sum_{i=1}^{n} \overline{K}WG_i . \overline{E}WG_i = \frac{1}{\overline{Y}Th} . \sum_{i=1}^{n} \overline{E}WG_i . \overline{Y}i_{tot} \\ \bar{i}_{bus} = \overline{Y}_{Th} .(\overline{E}_{Th} - \overline{V}_r) \end{cases} \tag{20}$$

If all induction machines and transformers have the same parameters, the equation (v) becomes:

$$\begin{cases} \overline{E}Th = \overline{E}i \\ \bar{i}bus = n.\overline{Y}i_{tot} .(\overline{E}i - \overline{V}r) \end{cases} \tag{21}$$

9. EXPERIMENTAL RESULTS

9.1. Case Study: Phase C of the Wind Farm of Sidi-Daoud

The "step C" of the Sidi-Daoud wind farm consists of 26 wind turbines (AE61) distributed over three branches.

Table 2
Step C of the wind farm Sidi-Daoud

branch	*WT number*	*Power (MW)*	*Distance from Substation (km)*
1C	9	11.880	1.560
2C	10	13.200	2.765
3C	7	9.240	0.770

The connection of the wind farm of Sidi-Daoud to high voltage grid is assured in two steps. The first step from 690 V to 30 kV by a transformer (LV/MV) for each wind turbine (at the tower foot) and the second step from 30 kV to 90 kV by a external transformer (MV / HV) via an underground cable [13].

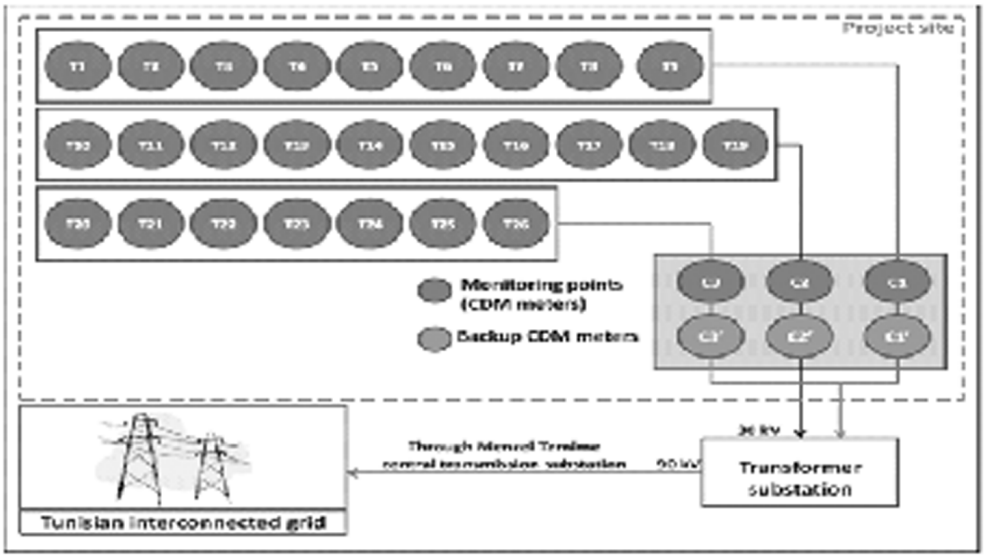

Figure 11: Configuring phase C of wind farm of Sidi-Daoud

10. RESULTS AND DISCUSSION

The aggregation of "step C" of wind farm Sidi-Daoud is performed in three steps. The first step is the aggregation of each branch (1C, 2C and 3C); the second step is the aggregation of equivalent wind turbines of branches 1C and 3C (connected to same bus); finally, the aggregation of the overall of wind turbines (connected to the network bus).

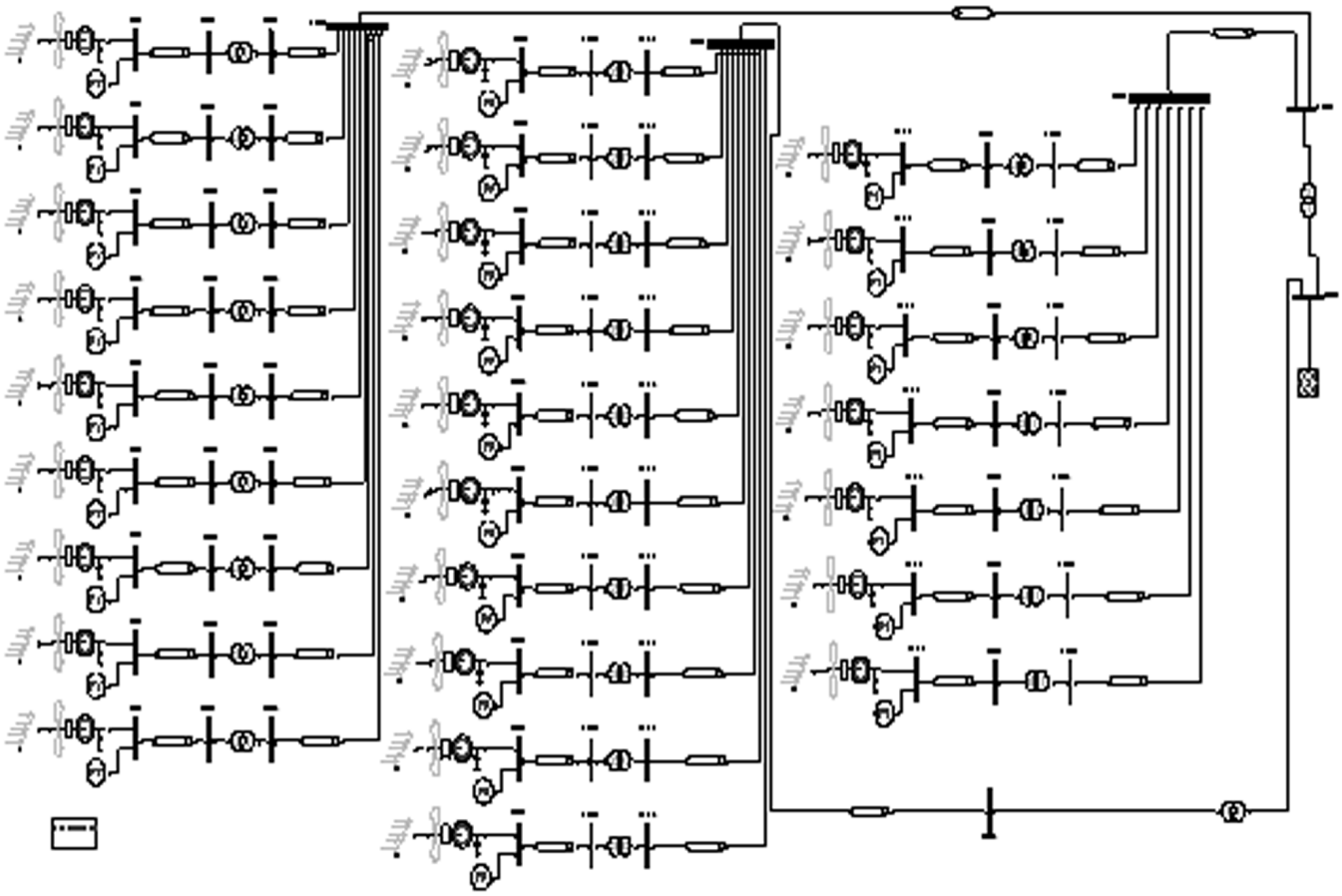

Figure 12: Configuration of the phase C of wind farm of Sidi- Daoud under PSAT

Figure 10 shows the "step C" configuration of wind farm of Sidi-Daoud simulated under PSAT software.

Figure 13 shows the first step of aggregation where wind turbines of branches (1C, 2C and 3C) are replaced by their equivalent wind turbines. Equivalent winds turbines of branches 1C and 3C are connected to the same bus are replaced by an equivalent wind turbine (second step of aggregation).

In this step, we replaced all the "step C" of wind farm Sidi-Daoud by an equivalent system (wind turbines and distribution systems) connected to the network bus "Figure 14".

The simulations are performed in the time domain for a Weibull wind model applied to branches (1C, 2C and 3C). The following figures show the simulation results from a few algebraic and dynamic variables before and after aggregation.

Table 3 gives the simulation results of active and reactive powers generated by the different wind turbines in static regime before aggregation.

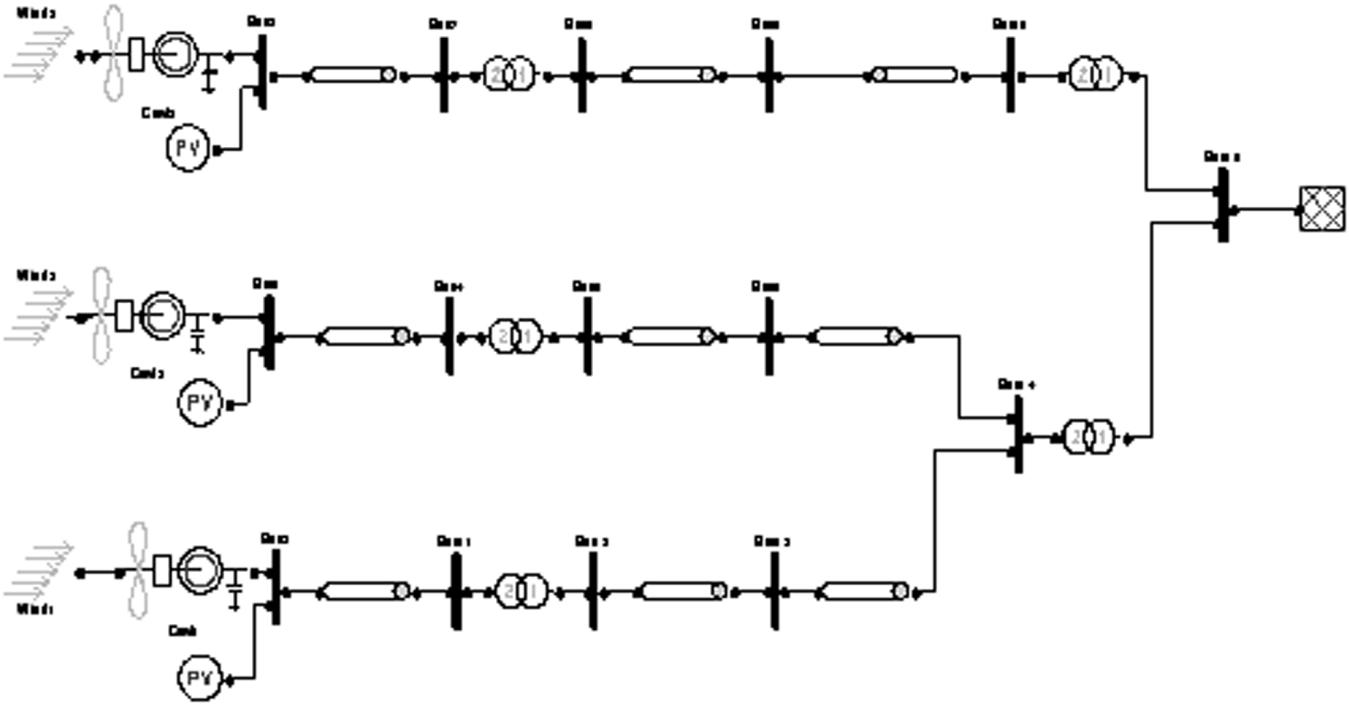

Figure 13: First aggregation step

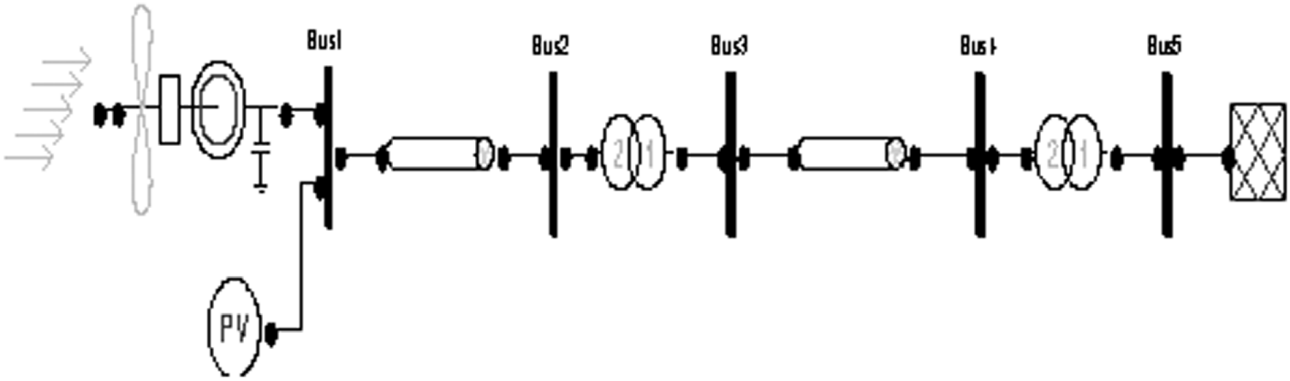

Figure 14: The equivalent wind turbine of step C of wind farm Sidi-Daoud

Table 3
The results of active and reactive power in the steady state for phase C

N° AG	Wind speed (m/s)	Active power (pu)	Reactive power (pu)	N° AG	Wind speed (m/s)	Active power (pu)	Reactive power (pu)
1	7.1	0.2171	-0.06859	14	6.5	0.164	-0.02004
2	7.8	0.2855	-0.14931	15	7.2	0.2265	0.09331
3	6.8	0.1898	-0.03664	16	5.6	0.09653	-0.06136
4	8.5	0.3587	-0.2329	17	5.9	0.1172	0.03566
5	7.5	0.2555	-0.11519	18	5.1	0.0664	0.09785
6	5.7	0.1032	0.06742	19	5.5	0.09007	0.06821
7	6.6	0.1724	-0.01706	20	5.5	0.09007	0.08589
8	6.4	0.1557	0.00275	21	7	0.2079	-0.05709
9	4.3	0.02995	0.15743	22	6.2	0.1397	0.02463
10	5.7	0.1101	0.04671	23	7.7	0.2754	-0.13726
11	4.8	0.05102	0.11935	24	6	0.1245	0.04256
12	7	0.2079	-0.0719	25	6.5	0.164	-0.00566
13	5	0.06105	0.10624	26	7.7	0.2754	-0.13819

Figure13 represents the simulation (time domain) of a Weibull wind (lines 1C, 2C and 3C) for first and final aggregation step.

The simulation results (Figure 15) shows that the wind speed of the equivalent wind turbine (Final Aggregation (F Ag)) is the average speed of three equivalent wind turbines (line 1C, 2C and 3C).

The following Figures show the simulation results from a few state variables of system studied before and after aggregation.

Figures 16(a) and 16(b) respectively show the results of simulation of the emf the direct and quadrature axis for the equivalent generators of the first aggregation step and the equivalent generator of the final aggregation. As the machines are identical and that the wind turbines speeds are considered uniform the gap between the e.m.f. are low ($\approx 10^{-3}$ pu near).

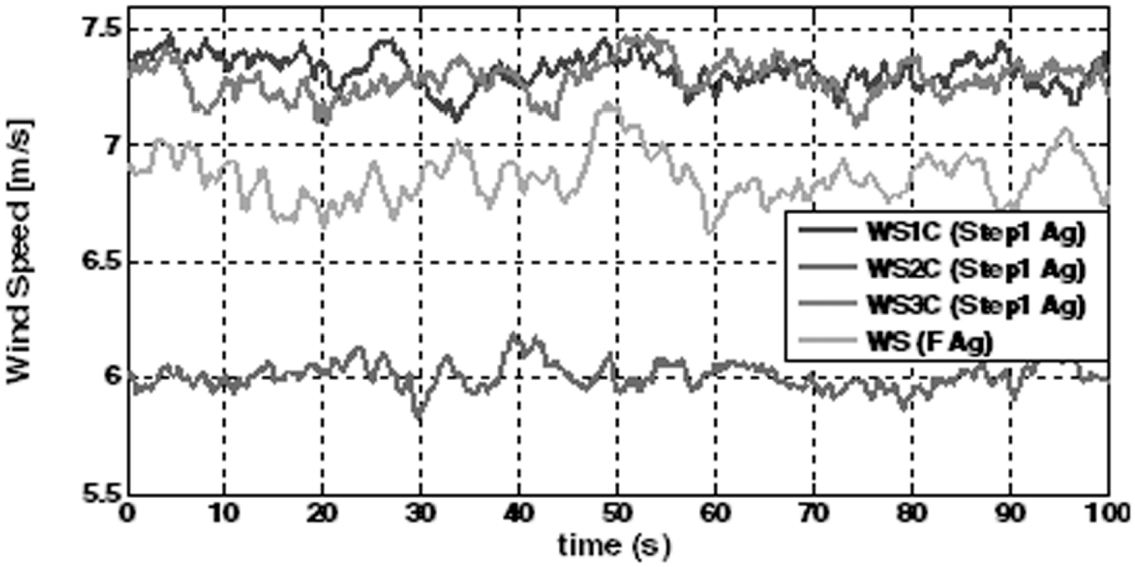

Figure 15: Wind speed

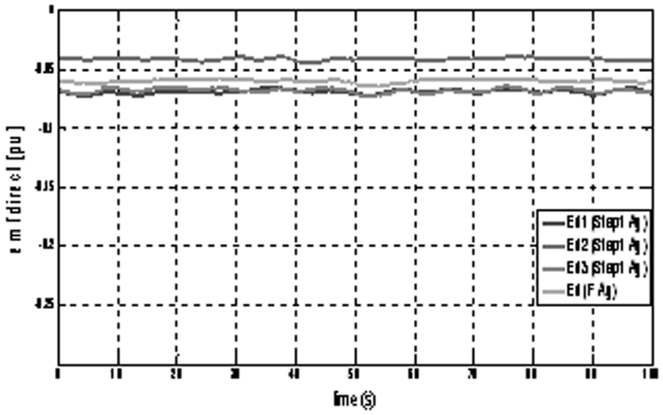

Figure 16(a): emf direct axis

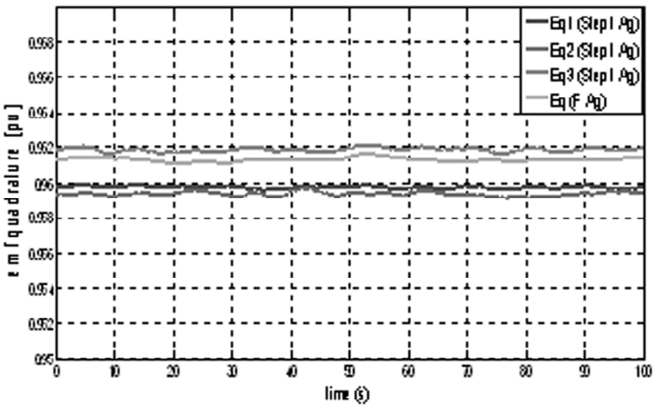

Figure 16(b): emf quadrature axis

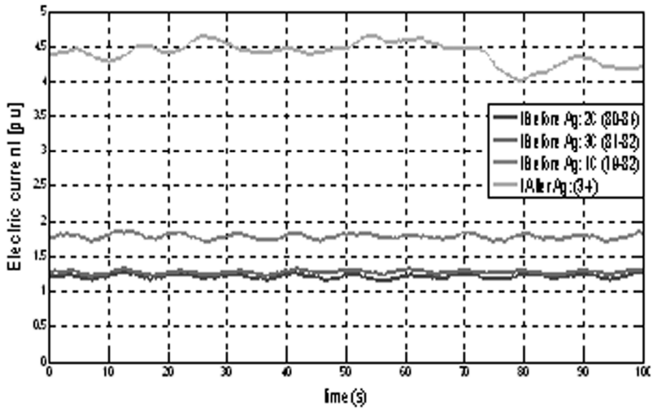

Figure 17(a): Current before and after aggregation

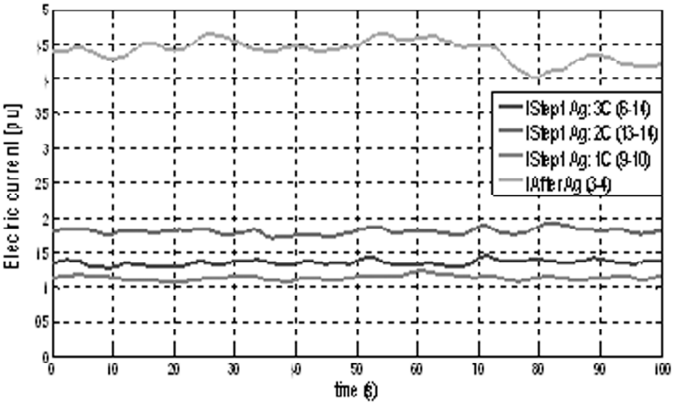

Figure 17(b) : Current first and final step aggregation

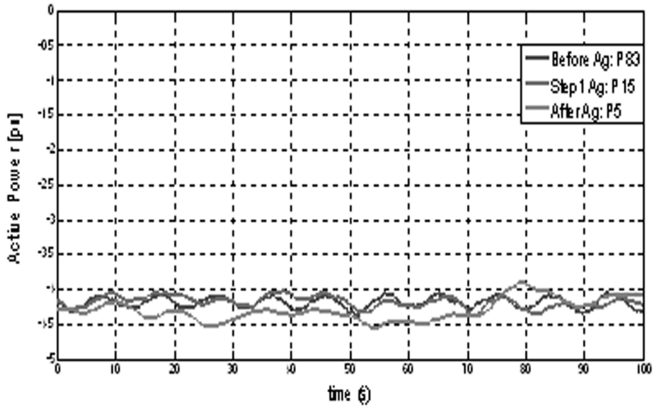

Figure 18(a) : Active power to the grid bus for the three case study

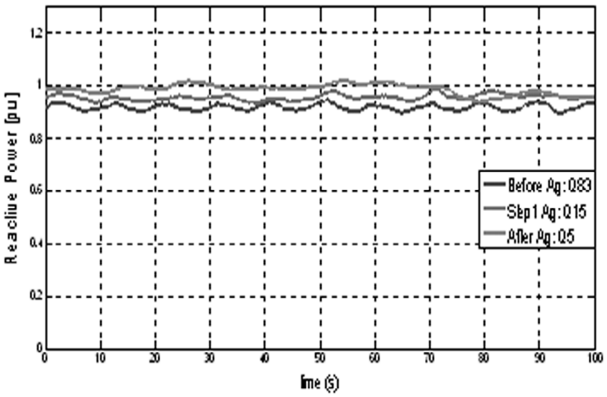

Figure 18(b) : Reactive power to the grid bus for the three case study

Figure 17 (a) shows the current injected by the wind turbines of lines (1C, 2C and 3C) before aggregation and the total current after full aggregation. While Figure 15(b) shows the currents injected by the equivalent generators of three lines (step1 aggregation) and the total current injected by the equivalent generator (final aggregation). These results show that total current injected by the Phase C is almost equal to the total currents supplied by the lines (1C, 2C and 3C) before and after aggregation.

Figures 18 (a) and 18(b) represent respectively the active and reactive power to the network node for the three states of phase C. We notice that the gap between the different powers is weak this is due to respect of aggregation procedures.

Figures 19(a) and 19(b) represent respectively the active and reactive power to the network before and after final aggregation as well as those transited by the three lines (1C, 2C and 3C) before aggregation.

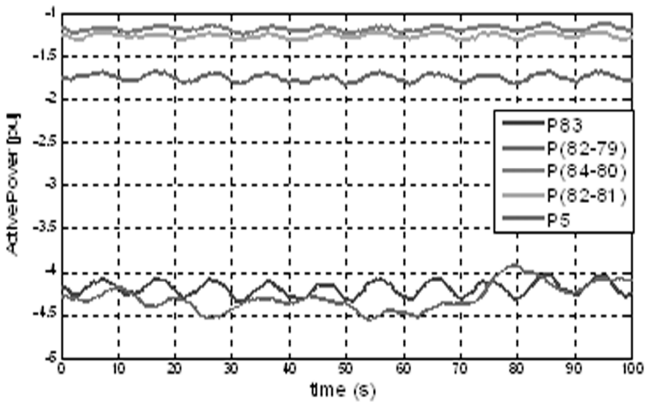

Figure 19(a): Active power before and final aggregation

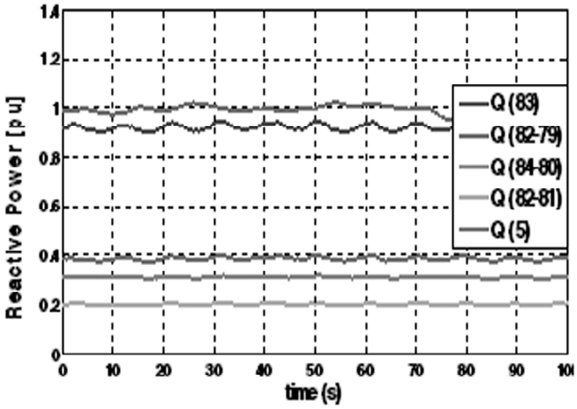

Figure 19(b): Reactive power before and final aggregation

The simulation results show that the difference is small between the electrical variables of the wind turbine system before and after aggregation. This difference is due to the fact that before aggregation we work with a real detailed system but after aggregation we work with a fictional equivalent system based on assumptions which may generate errors.

11. CONCLUSION

In this study the simulation results show that if the wind speed across the wind farm is uniform and that wind turbines are of the same type, the dynamics of the whole of wind turbines can be represented by a simple equivalent model of a single wind turbine connected to the network via a distribution system equivalent (cables and transformers). Indeed, the aggregation of a wind farm has the advantage of facilitated the study enormously, reduce the order of the system and by consequently the simulation time.

In this case study, we used the case of fixed speed wind turbines with cage induction machine connected directly to the grid. Indeed, the aggregation can be carried out for wind turbine systems case with variable speed connected to network via a interfaces (static converters). In this case, the converter must have a dimension corresponding to the power generated by the equivalent wind turbine.

APPENDIX

Table 4
Wind turbines parameters

Parameters		*Value*
Rated Power	P (MW)	1.320
Nominal Wind Speed	V_n (m/s)	16
Wind Turbine Bus Voltage	V_n (V)	690
Grid Frequency	F (Hz)	50
Stator Resistance	R_S (pu)	0.0097
Stator Leakage Reactance	X_S (pu)	0.1284
Rotor Resistance	R_r (pu)	0.0108
Rotor Leakage Reactance	X_r (pu)	0.1284
Magnetization reactance	X_m (pu)	5.579
Turbine inertia constant	H_t (s)	5
Generator inertia constant	H_g (s)	3.7146
Shaft stiffness	K_S (pu)	70

Table 5
Transformer parameters

Parameters		*T (MV) (0.69/30kV)*	*T (HV) (30/90kV)*
Nominal Power	S (MVA)	1.6	40
Primary Resistance	R_1 (pu)	0.000265	≈0
Secondary Resistance.	R_2 (pu)	0.000265	≈0
Primary leakage inductance	x_1 (pu)	0.0155	0.06
Secondary leakage inductance	x_2 (pu)	0.0155	0.06
Résistance magnetizing resistance	R_m (pu)	34.144	100
Magnetizing Inductance	x_m (pu)	11.7605	10

Table 6
Line parameters

	Parameters	*Value*
Line resistance	R_{MV} (Ω/Km)	0.272
Line reactance	X_{MV} (H/Km)	0.08/100π
Line resistance	R_{HV} (Ω/Km)	0.159
Line reactance	X_{HV} (H/Km)	0.138 /100π

REFERENCES

[1] F. Bacha and R. Karoui, "Simulation of a Wind Farm of Sidi-Doud–Tunisia Using PSAT, " *Prof. 2003 International Conference on Electrical Engineering and Software Applications*, Hammamet, Tunisia, **ICEESA-2003**, 1-7, 2003.

[2] F. Ben Amar, M. Elamouri and R. Dhifaoui, "Energy assessment of the first wind farm section of Sidi-Daoud, Tunisia", *Renewable Energy*,**33** (10), 2311-2321, 2008.

[3] F.Sada,*Aggregate Model of Large Wind Parks for Power System Studies*,Master's Thesis, KTH Electrical Engineering, Stockholm, Sweden, March 2011.

[4] Y.U. Lopez and J.A.D. Navarro, "Small signal stability analysis of wind turbines with squirrel cage induction generators," *Proc. 2008 IEEE Transmission and Distribution Conference and Exposition: Latin America* , Bogota, Colombia, **TDC-LA-2008**, 1-10, 2008.

[5] A. Karakas, M.H. Kao, F. Li and S. Adhikari, "Aggregation of multiple induction motors using MATLAB-based software package," *Proc. Power Systems Conference and Exposition*, Seattle, USA, **PSCE-2009**, 1-6, 2009.

[6] N. Hatziargyriou, M. Donnelly, J.A. Pecas Lopes, M. Takasaki, H. Chao and R. Lasseter, *Modeling New Forms of Generation and Storage*, Cigre Technical Brochure, November 2000.

[7] W. Qiao, R.G. Harley and G.K. Venayagamoorthy, "Dynamic modeling of wind farms with fixed-speed wind turbine generators,"*Proc. Power Engineering Society General Meeting*, **PES-2007**, 1-8, 2007.

[8] E.G. Potamianakis and C.D. Vournas, "Aggregation of wind farms in distribution networks," *Proc. European Wind Energy Conference*, Madrid, **EWEC-2003**, 1-7, 2003.

[9] K.B. Kilani and M. Elleuch, "Simplified modelling of wind farms for voltage dip transients," *Proc. International Multi-Conference on Systems, Signals and Devices*, Chemnitz, Germany, **SSD-2012**, 1-6, 2012.

[10] E. Muljadi, C.P. Butterfield,A. Ellis, J. Mechenbier, J. Hochheimer, R. Young, N. Miller, R. Delmerico, R. Zavadil and J.C. Smith, "Equivalencing the collector system of a large wind power plant," Proc. IEEE Power Engineering Society General Meeting, Montreal, Canada, **PES-2006**, 2006.

[11] F. Gonzalez-Longatt, P. Regulski, P. Wall and V. Terzija, "Procedure for estimation of equivalent Model Parameters for Wind Farm using Post-Disturbulance on-line Measurement Data" *Proc. 2nd IEEE PES International Conference and Exhibition on Innovative Smart Grid Technologies,* Manchester,U.K., **ISGT Europe-2011**,1-7, 2011.

[12] A. Perdana, *Wind Turbine Models for Power System Stability Studies*,Master's Thesis,Department of Energy and Environment, Chalmers University of Technology, Goteborg, Sweden, 2006.

[13] Tunisian Company of Electricity and Gas, "Réalisation d'une ligne électrique aérienne 90 KV/Sidi Daoud/Menzel Temime,"*Enviserv Consult*, July 31, 2009.

[14] S. Driss, B. Faouzi and D. Rachid, "Analysis of an induction generator connected to infinite bus system,"*Proc. International Aegean Conference on Electrical Machines and Power Electronics*, Bodrum, Turkey, ACEMP-2007, 701-706, 2007.

[15] S. Vaidyanathan, "A novel 3-D conservative chaotic system with sinusoidal nonlinearity and its adaptive control", *International Journal of Control Theory and Applications*, **9** (1), 115-132, 2016.

[16] S. Vaidyanathan and S. Pakiriswamy, "A five-term 3-D novel conservative chaotic system and its generalized projective synchronization via adaptive control method", *International Journal of Control Theory and Applications*, **9** (1), 61-78, 2016.

[17] S. Vaidyanathan, K. Madhavan and B.A. Idowu, "Backstepping control design for the adaptive stabilization and synchronization of the Pandey jerk chaotic system with unknown parameters", *International Journal of Control Theory and Applications*, **9** (1), 299-319, 2016.

[18] A. Sambas, S. Vaidyanathan, M. Mamat, W.S.M. Sanjaya and R.P. Prastio, "Design, analysis of the Genesio-Tesi chaotic system and its electronic experimental implementation*", International Journal of Control Theory and Applications*, **9** (1), 141-149, 2016.

[19] S. Vaidyanathan and A. Boulkroune, "A novel hyperchaotic system with two quadratic nonlinearities, its analysis and synchronization via integral sliding mode control," *International Journal of Control Theory and Applications*, **9** (1), 321-337, 2016.

[20] S. Sampath, S. Vaidyanathan and V.T. Pham, "A novel 4-D hyperchaotic system with three quadratic nonlinearities, its adaptive control and circuit simulation," *International Journal of Control Theory and Applications*, **9** (1), 339-356, 2016.

[21] A.T. Azar and S. Vaidyanathan, *Chaos Modeling and Control Systems Design*, Springer, Berlin, 2015.

[22] I. Pehlivan, I.M. Moroz and S. Vaidyanathan, "Analysis, synchronization and circuit design of a novel butterfly attractor", *Journal of Sound and Vibration*, **333** (20), 5077-5096, 2014.